NUMERICAL ANALYSIS OF FRETTING PROBLEM IN FUEL ROD OF A PWR NUCLEAR REACTOR

Silvana Carreiro de Oliveira, silvana_carreiro@id.uff.br [1]
Luiz Carlos Rolim Lopes, luiz.crolim@uol.com.br [1]
Césio Túlio Alves dos Santos, césiosantos@id.uff.br[1]

[1] Escola de Engenharia Industrial Metalúrgica de Volta Redonda, Programa de Pós-Graduação em Engenharia Mecânica, Universidade Federal Fluminense, Avenida dos Trabalhadores, 420, CEP 27255-125, Volta Redonda-RJ, Brazil

Abstract. *One of the major causes of failure in a nuclear plant is the fretting problem in the fuel rod. Due to this, several experimental studies have been conducted in the last years to observe more about the phenomenon and predict when and in what location of structure fretting failure can possibly happens. One of the frequent occurrence of fretting in PWR nuclear reactors is the contact region between the spacer grid and fuel rod and happens because of flow-induced vibration. This work aims to characterize this region of contact through the finite element method, with the help of Abaqus application. For this, a simplified model of PWR fuel assembly was used and fretting simulations was performed for different rod displacement. In the model definition, the properties of the spacer grid and the fuel cladding materials (Inconel-718, produce by cold rolling and machining and the Zircaloy-4, made by extrusion, respectively) were used. Simulations allowed obtaining the stress state at the contact region, such as contact pressure and shear stress distribution along the contact surface, the size of this contact and the stick region for each different situation. To validate the model, a comparison between the numerical results obtained in computer simulation and the theoretical results derived from formulas of contact mechanics; mainly by the Hertz contact theory was done. In the contact region with the springs, the numerical results for the contact size changed by 10% and for the contact pressure, this variation was around 30% compared with the theoretical results. In the contact region with the dimples, the variation of the contact size was 10%, while the variation of the contact pressure ranged 20%. This comparison showed that the numerical results are in agreement with the theory, making the model valid.*

Keywords: *fuel fretting, finite element method, contact mechanics*

1. INTRODUCTION

A very common damage in nuclear power plants is due to fretting process and if it has not been treated correctly can causes major failures in the fuel assembly. Fretting, that is, small amplitude oscillatory displacement between surfaces in contact, is a phenomenon observed in many mechanical assemblies and can significantly reduce the life of an assembly. Depending on the imposed forces and relative displacements, the resulting damage may be wear (material removal), fatigue (cracking) or both (Ding et al., 2008). The cyclic loads cause small relative tangential displacements between the bodies, which, over the history of the loading, may be able to form small cracks near the contact region, and their consequent propagation, which may lead to failure of the component. These small displacements, along with the cyclic loads, generate a multiaxial state of stress, with varying mean stress and high gradients and stress peaks, besides a local plastic deformation. These described conditions can accelerate the local damage process and cause premature cracking.

The fretting problem is studied by the approach of Contact Mechanics and is a complex tribological problem, which depends on different parameters having influence on response of connected surfaces, such as:. Coefficient of Friction (COF), roughness, slip amplitude, environmental conditions and so on. Each of these parameters has significant impact on fretting and fretting fatigue response of material (Talemi, R. H., 2014). Under fretting conditions, the contact zone is divided in two parts: slip and stick regions, as shown in Fig. 1.

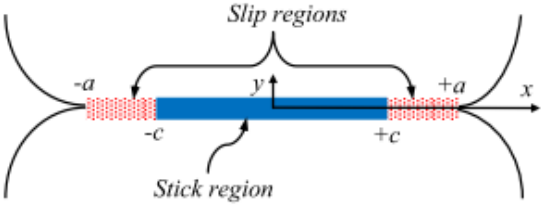

Figure 1. By applying tangential load the contact area is divided into slip and stick zones. (Talemi, R. H., 2014)

In the case studied in this paper, the fretting occurs in the region of contact between the spacer grid (made of Inconel-718) and the fuel rod cladding of a PWR nuclear power plant reactor (made of Zircaloy-4) and, according to Hyung-Kyu et. Al. (2006) its primary cause is a flow-induced vibration (FIV) due to reactor coolant flow. By vibrating, the fuel rods generates shear and slip forces between the two surfaces, which causes oscillatory relative motion in this region, which is nothing more than the definition of fretting itself. The fuel rods are supported in a fuel assembly by the friction forces between springs or dimples of spacer grids. (Hyung-Kyu, 1999) Figure 2 shows the configuration of this contact situation between the fuel rod and the spacer grid.

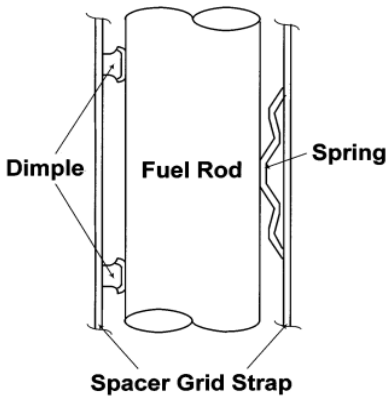

Figure 2. Configuration of the line contact between fuel rod and spacer grid. (Hyung-Kyu, 1999)

As an experimental study of this phenomenon is difficult to perform, so the present study was carried out by means of numerical modeling using the Finite Element Method (FEM).

2. METHODOLOGY

As previously stated, the work consists in performing simulations through the FEM and its results have been compared with the theoretical results obtained by the Hertz contact theory. This method has a high level of accuracy, which makes it quite reliable. The FEM application used in this work is the ABAQUS/Explicit academic research version 6-9. The following topics will describe the development of the theory and computational model used to describe the problem.

2.1. Materials Studied

As previously stated, the fuel rod is made of Zircaloy-4, which is a zirconium alloy and the spacer grid is made of Inconel-718, which belongs to the Ni–Cr based superalloys family.

The main reason for the choice of a zirconium alloy are the strength/toughness requirements for the pressure boundaries, good liquid corrosion resistance and neutronics. The demands coming from new nuclear plants need structural materials with better performance at higher temperatures and higher doses in environments different from water. Finally, or even primarily all improvements have to be made at affordable costs. (Hoffelner, 2013) The fuel rods for nuclear reactors are manufactured by extrusion of the zirconium-based alloy and cold rollings of the extruded product with annealings

Already the choice of Inconel alloy for the manufacture of the spacer grid is due to the fact it has a good cryogenic properties, good fatigue and mechanical strength at moderate temperatures and relatively good creep behavior. In addition, Ni and Cr provide resistance to corrosion, oxidation, carburizing and other damage mechanism acting at high temperature. (Thomas et al., 2006) The Inconel 718 can be machined in either the annealed or the age-hardened condition, which gives better chip action on chip breaker tools and produces a better finish.

2.2. Theoretical Analysis of the Problem

Since sliding displacements and internal stresses can only be analyzed from the use of contact stresses, the study of the problem of fretting in the fuel rod is carried out from the point of view of contact mechanics. The actual contact between two surfaces is often complex. Typically, three types of representative contact can be used: sphere/plane, cylinder/plane and surface/plane. The contact type in the fuel fretting problem is the cylinder/plane.

According to Nowell et al. (2006), stress gradients are likely to be very high, due to the localised stress concentration at the contact. The magnitude of these stress gradients is usually much higher than those associated with typical design features of components. Bramhall (1973) was the first to investigate the size effect in a systematic way by

noting that the peak pressure, p_0 , in a cylindrical Hertzian contact is related to the normal load, *p*,and the pad radius, r, by

$$p_0 = \sqrt{\frac{pE^*}{\pi r}} \tag{1}$$

where E^* is a constant for the material pair, and is given by

$$E^* = \left(\frac{1-\nu_1^2}{E_1} + \frac{1-\nu_2^2}{E_2}\right)^{-1} \tag{2}$$

where ν is the Poisson's ratio and *E* the Young's Modulus. The subscripts 1 and 2 refer to fuel rod cladding and spring/dimple geometry, respectively. The semi-width of the contact, a, is given by

$$a = \sqrt{\frac{4pR_{eq}}{\pi E^*}} \tag{3}$$

where R_{eq} is given by

$$\frac{1}{R_{eq}} = \frac{1}{r_1} + \frac{1}{r_2} \tag{4}$$

Once again, the subscripts 1 and 2 refer to fuel rod cladding and spring/dimple geometry, respectively. The spring and dimple radius was considered to be infinite, so the second term of Eq. (4) is zero. It is worth mentioning that the proposed model in this paper does not completely obey the Hertz contact conditions, therefore, theoretical values are only approximations. Table 1 shows the material properties that will be use in this present work.

Table 1. Mechanical properties of materials

Property	Inconel-718	Zircaloy-4
Elastic Modulus (MPa)	200000	100000
Density (kg/m$^{3)}$	8300	9309,5
Poisson's ratio	0.295	0.35

These properties shown in the Tab. (1) will also be used in the computational model. In order to compare the numerical (φ) and analytical (φ) results, the error between these values is calculated by the absolute error ($E(\varphi)$) and relative error (E_r) errors, which are given by Eq. (5) and Eq. (6), respectively:

$$E(\varphi) = \phi - \varphi \tag{5}$$

$$E_r = \frac{E(\varphi)}{\phi} \tag{6}$$

2.3. Finite Element Model

Was adopted the Finite Element Method to perform this work due to the high degree of complexity of the problem, which involves both partial slip and total slip. In addition, this method has a high level of accuracy, which makes it quite reliable.

In this work, were used a simplified two-dimensional model of the contact region between the rod and the springs and another one to represent the contact between the rod and the dimples. For this, was made a cut in the plane in which the rod comes in contact with the springs and another cut in the plane in which it with the dimples

In the realization of the model, it is necessary to define what kind of interaction between the contact surfaces will be used. The definition that Abaqus (2009) makes for the contact between two bodies is that they are two surfaces that can interact. In this work, the algorithm called master-slave was used. Another necessary definition is the friction formulation and Litewka (2005) stated that for the fretting problem, the models that best fit are the Lagrange Multiplier method and the Penalty method. Studies shows that the Lagrange Multiplier method has better results, but the

computational cost is higher compared to the Penalty method. Because of that, was chosen the Penalty method and the coefficient of friction is equal to 0.4.

This model consists of two steps. The first will be an application of a displacement (indentation) of 0.001 mm at x and y directions on the surface of the fuel cladding to ensure contact and aims to characterize the contact before the cyclic displacement is applied. The second one will be to simulate the fretting phenomenon by applying two different cyclic displacement: 0.01 mm and 0.005 mm. in x and y directions. On the other hand, the loads applied in the model are the internal pressure in the fuel rod due to uranium fission and an external pressure, which is the operating pressure of the nuclear reactor. The external pressure is equal to 1.55 MPa and will be used three different values for internal pressure: 8.27 MPa, 15 MPa and 20 MPa.

The generated mesh was refined in de contact regions as elements of four different sizes: 10 μm, 5 μm, 3 μm and 1 μm. Convergence tests were carried out to find that element size presented the best result taking into account the relative error compared to the analytical result and the computational time spent to complete the simulation. It was observed that for the contact between rod and spring, the best size was 3 μm and for the contact between rod and dimple the chosen size was 5 μm. The element used in the contact region was the CPS4R, which is a quadratic, two-dimensional, four-node element that uses reduced integration. In the other regions, was used the element CPS3, which is a triangular element with three nodes according to ABAQUS/Explicit terminology. Both elements are linear. Figure 3 shows the adopted mesh to represent the contact region, emphasizing the region where the mesh was refined.

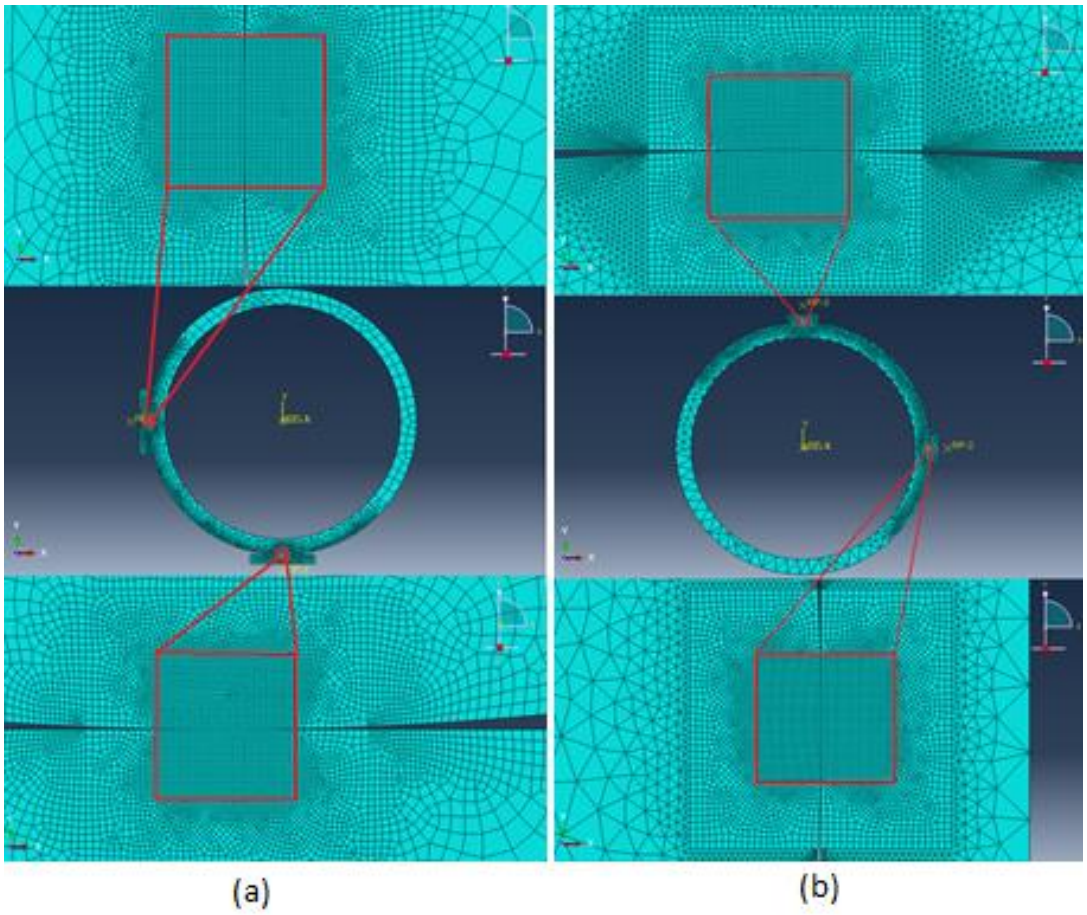

Figure 3. Adopted finite element mesh for the contact region: (a) between fuel rod and spring (b) between fuel rod and dimples.

3. RESULTS AND DISCUSSION

Firstly, was performed an analysis of the behavior of the contact region before the cyclic displacement where the contact characteristics were studied in terms of contact size ($2a$) and maximum pressure (p_0) along the contact size for each internal pressure applied in the model. A comparison between the theoretical and numerical values of these parameters for different internal pressures and the errors obtained for the rod/spring model and for the rod/dimples model is shown in Tab. 2 and Tab. 3, respectively. The values of the theoretical parameters were calculated through Eq. (1) and Eq. (3) and the errors were calculated through Eq. (5).

Table 2. Comparative between the numerical and theoretical values of the contact size and the maximum pressure at the contact region of the spring and their respective errors.

	Internal pressure (MPa)	Contact feature	Theoretical value	Numerical value	Error (%)
Low spring	8,27	$2a$ (mm)	0.0731	0.0781	6.97
		p_0 (MPa)	144	240	66.51
	15	$2a$ (mm)	0.0984	0.1022	3.84
		p_0 (MPa)	194	265	36.65
	20	$2a$ (mm)	0.1136	0.1202	5.79
		p_0 (MPa)	224	272	21.15
Side spring	8,27	$2a$ (mm)	0.0731	0.0686	6.09
		p_0 (MPa)	144	232	61.29
	15	$2a$ (mm)	0.0984	0.0925	6.02
		p_0 (MPa)	194	262	35.21
	20	$2a$ (mm)	0.1136	0.1163	2.38
		p_0 (MPa)	224	273	21.72

Table 3. Comparative between the numerical and theoretical values of the contact size and the maximum pressure at the contact region of the dimple and their respective errors.

	Internal pressure (MPa)	Contact feature	Theoretical value	Numerical value	Error (%)
Upper dimple	8,27	$2a$ (mm)	0.0731	0.0650	11.09
		p_0 (MPa)	144	172	19.63
	15	$2a$ (mm)	0.0984	0.0799	18.78
		p_0 (MPa)	194	206	6.10
	20	$2a$ (mm)	0.1136	0.0999	12.08
		p_0 (MPa)	224	208	7.36
Side dimple	8,27	$2a$ (mm)	0.0731	0.0700	4.25
		p_0 (MPa)	144	172	19.61
	15	$2a$ (mm)	0.0984	0.0949	3.54
		p_0 (MPa)	194	203	4.85
	20	$2a$ (mm)	0.1136	0.0949	16.49
		p_0 (MPa)	224	216	3.46

Through the results presented in Tab. 3 and Tab. 4, it was observed that the contact size presents errors with satisfactory values and the contact pressure presents large errors, since, as said before, the model does not completely obey the Hertz condition. It is also possible to observe that as the internal pressure increases, the error shown for the maximum pressure value decreases. Figure 4 shows the pressure distribution ($p(x)$) profiles along the contact size for each situation studied and it can be seen that, as expected, by increasing the internal pressure in the rod, the contact size and the maximum pressure also increase. However, it is also observed that the maximum pressure values have a smaller variation than the contact size for each internal pressure applied.

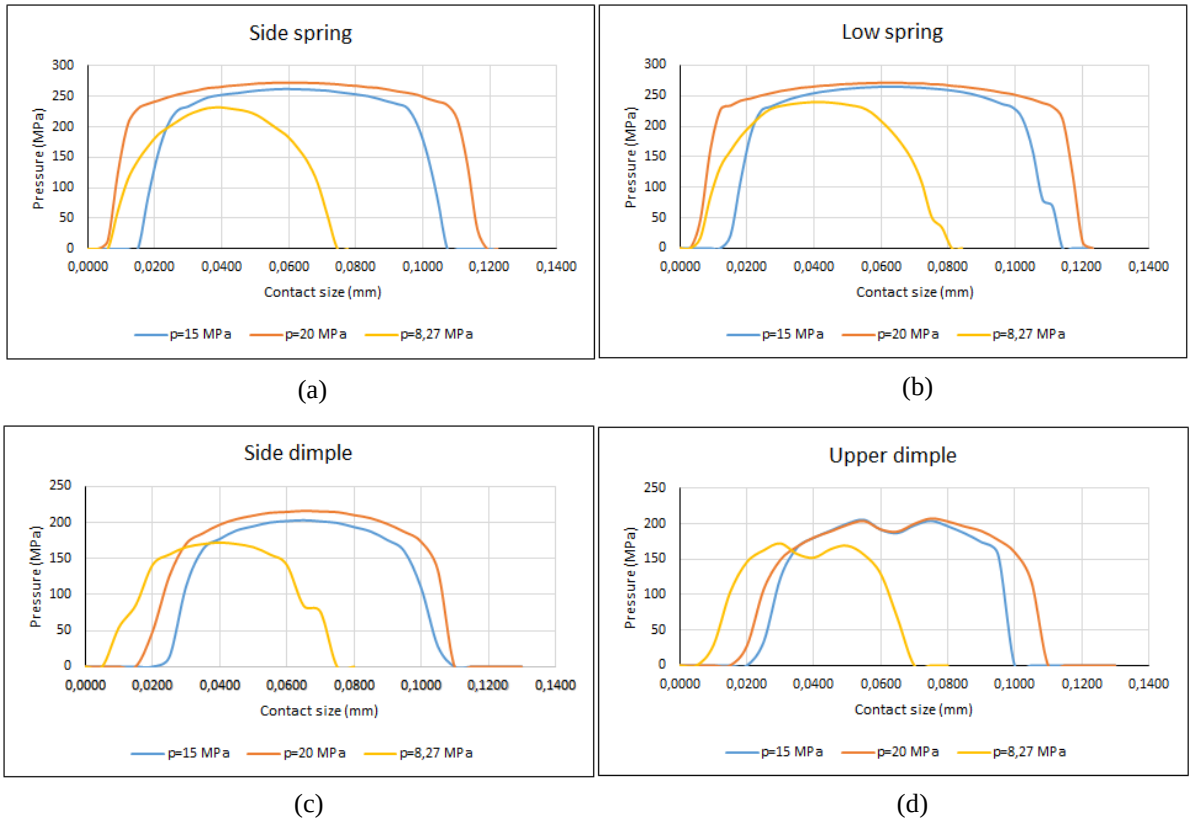

Figure 4. Pressure distribution along contact size before the fretting simulation: (a) for the side spring (b) for the low spring (c) for the side dimple (d) for the upper dimple.

After the characterization of the contact region, the cyclic displacement was applied in the model in order to observe what happens at the end of this process. In this step, the objective is to obtain the shear stress ($q(x)$) curve along the contact size in order to verify the size of the stick zone, in addition to the pressure distribution to obtain contact size and maximum pressure after the fretting simulation. The contact features obtained numerically are shown in Tab. 4 and Tab. 5.

Table 4. Results of the contact features in the numerical rod/spring model for each internal pressure and displacement applied to the fuel rod

	Internal pressure (MPa)	Displacement (mm)	Contact feature		
			p_0 (MPa)	$2a$ (mm)	$2c$ (mm)
Low spring	8.27	0.01	169	0.0661	0.0451
		0.005	169	0.0631	0.0451
	15	0.01	178	0.0932	0.0481
		0.005	195	0.0902	0.0721
	20	0.01	193	0.1112	0.0631
		0.005	206	0.1112	0.0871
Side spring	8.27	0.01	169	0.0597	0.0418
		0.005	169	0.0597	0.0418
	15	0.01	175	0.0895	0.0388
		0.005	193	0.0805	0.0597
	20	0.01	189	0.1074	0.0567
		0.005	204	0.1014	0.0746

Table 5. Results of the contact features in the numerical rod/dimple model for each internal pressure and displacement applied to the fuel rod

	Internal pressure (MPa)	Displacement (mm)	Contact feature		
			p_0 (MPa)	$2a$ (mm)	$2c$ (mm)
Upper dimple	8.27	0.01	132	0.0700	0.0400
		0.005	137	0.0500	0.0250
	15	0.01	171	0.0799	0.0250
		0.005	176	0.0699	0.0550
	20	0.01	172	0.0799	0.0500
		0.005	177	0.0799	0.0649
Side dimple	8.27	0.01	142	0.0500	0.0200
		0.005	145	0.0500	0.0300
	15	0.01	180	0.0650	0.0450
		0.005	178	0.0700	0.0500
	20	0.01	190	0.0799	0.0549
		0.005	186	0.0799	0.0649

From the results presented in Tab. 4 and Tab. 5, it is possible to verify that the displacement variation does not cause variation in the characteristics analyzed for the pressure of 8.27 MPa and has a little influence for other pressures, where the greatest variation is only observed to the stick zone size. This variation can be explained because, according to Vingsbo and Söderberg (1988), the fretting conditions change as the amplitude of the displacement increases. Due to this, the next analyzes will be carried out only for the displacement of 0.01 mm. The contact size is defined as a range between the last node where $p(x)=0$ to the next one where $p(x)=0$. To obtain the stick zone size, were plotted the shear stress distribution curves ($q(x)$) and the distribution of the friction resistance limit (μP) in the same region, as shown in Fig. 5 (springs) and Fig. 6 (dimples). According to Hyung-Kyu, (1999), if the Coulomb law is followed, the shear stress is equivalent to or greater then the friction resistance limit when two contact bodies slide (termed as gross slip) and if the shear stress is less than the friction resistance limit, the bodies do not slide (stick region). These regions are also indentified in Fig. 5 and Fig. 6 and from them it is possible to observe that the stick zone size changes as the load also changes. It is also observed that the dimples and springs behave in different ways: in the springs the adhesion zone increases with the pressure decrease and in the dimples the opposite occurs, the adhesion zone is smaller for the lower internal pressure.

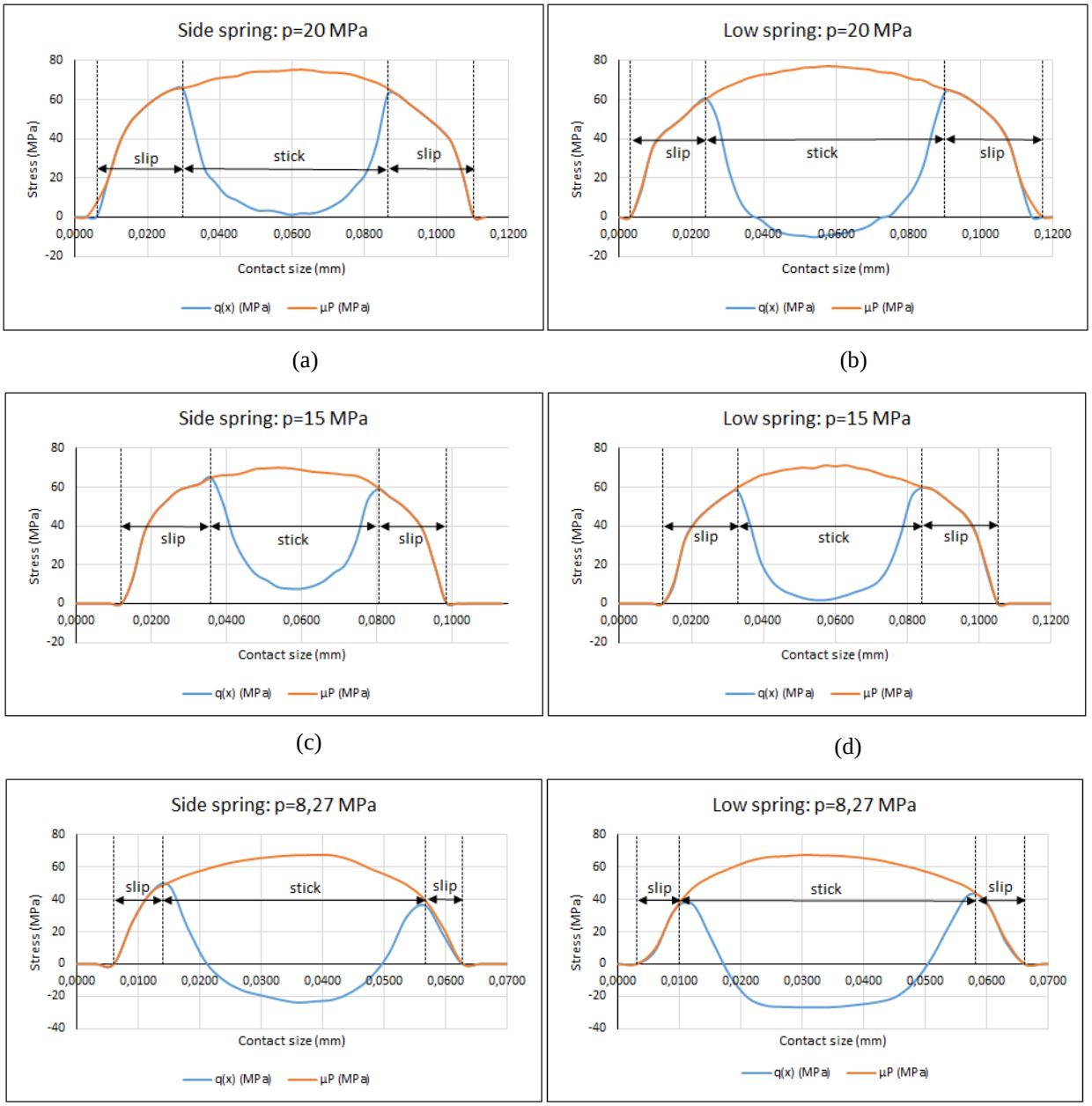

Figure 5. Distribution of the shear stress and the friction resistance limit along the contact size for the springs: (a) and (b) for pressure of 20 MPa; (c) and (d) for pressure of 15 MPa; (e) and (f) for pressure of 8.27 MPa.

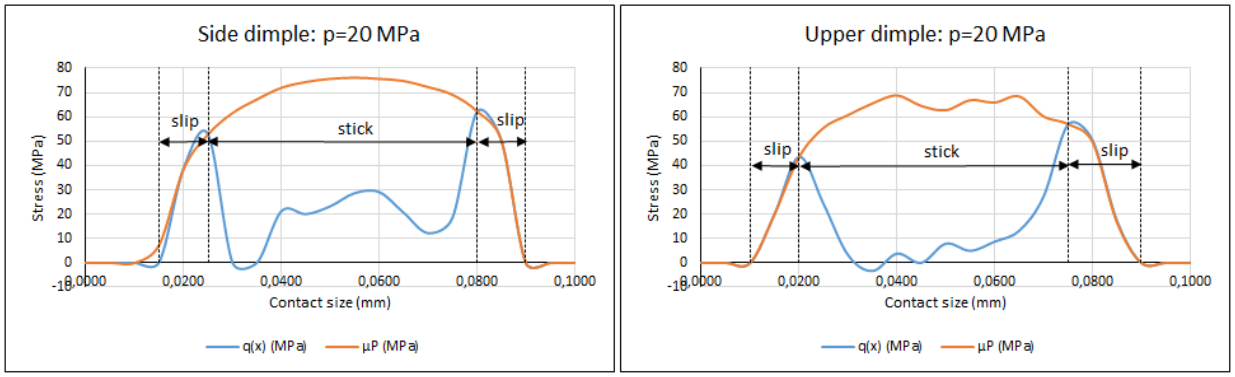

(a) (b)

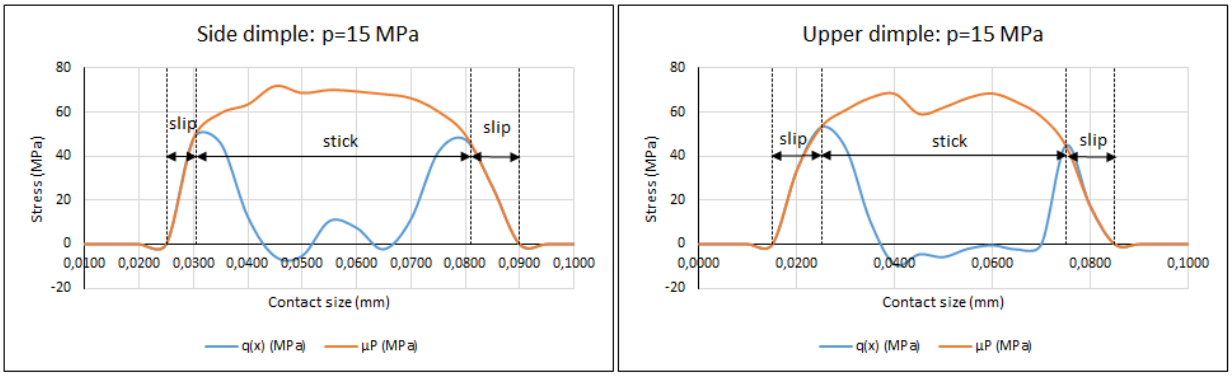

(c) (d)

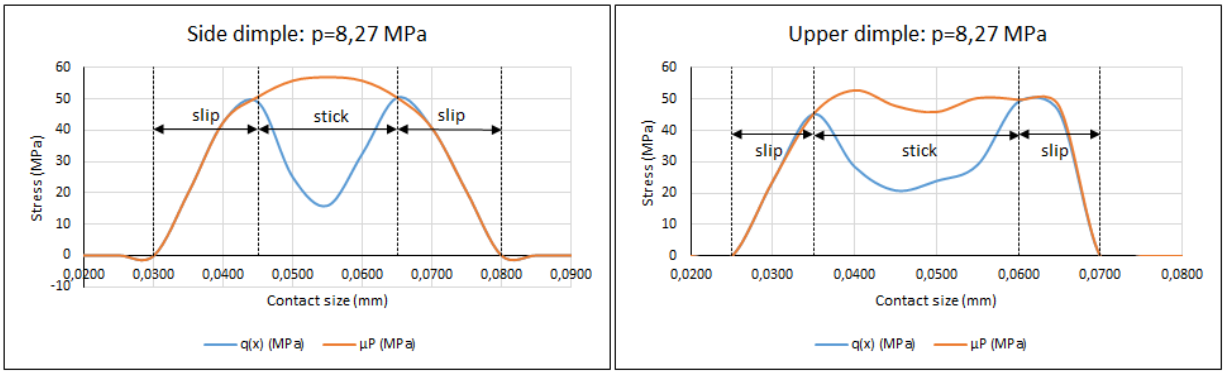

(e) (f)

Figure 6. Distribution of the shear stress and the friction resistance limit along the contact size for the dimples: (a) and (b) for pressure of 20 MPa; (c) and (d) for pressure of 15 MPa; (e) and (f) for pressure of 8.27 MPa.

4. CONCLUSION

Through the simulations performed to characterize the phenomenon of the fretting in the contact region between the fuel rod and the spacer grid of a fuel assembly, the following conclusions can be drawn:

- Although the model did not completely obey the Hertz theory, it has presented satisfactory results in relation to the contact size, whose errors were very small. Already, the maximum pressure presented a bigger error, but also satisfactory, since the formulas of Hertz did not apply totally to the model;
- After the fretting simulation, the contact features has changed, mainly the maximum contact pressure, which considerably decreased.
- With the increase of the displacement amplitude, was observed a change in fretting conditions, as expected.
- The change in internal pressure in the fuel rod has changed the contact zone size of the contact region and it was also observed that in contact with the springs, the stick zone is higher for lower pressures and in contact with the dimples, the stick zone is lower for the lower pressures.

5. ACKNOWLEDGEMENTS

The authors are grateful to CAPES and PROPPi/UFF for financial support to PGMEC-VR/UFF. Silvana Carreiro de Oliveira acknowledges CAPES and Eletronuclear for the financial support from CAPES/Electronuclear program.

6. REFERENCES

ABAQUS user's manual, 2009. Version 6-9, Dassault Systemes Simulia Corp., Providence, RI, USA.

Bramhall, R., 1973, "Studies in fretting fatigue", D.Phil. Thesis, University of Oxford.

Ding, J., Leen, S. B., Williams, E. J. and Shipway, P. H., 2008, "Finite element simulation of fretting wear-fatigue interaction in spline couplings", Tribology, 2, pp. 10-24.

Hoffelner, W., 2013, "Materials for Nuclear Plants", Ed. Springer, pp.81-82

Hyung-Kyu, K., 1999, "Mechanical analysis of fuel fretting problem", Nuclear Engineering and Design, 192, pp. 81-93

Hyung-Kyu, K., Young-Ho, L., Sung-Pil, H., 2006, "Mechanical and experimental investigation on nuclear fuel fretting", Tribology International, 39, pp. 1305-1319.

Litewka, P., 2005, "The penalty an lagrange multiplier methods in the frictional 3D beam to beam contact problem", Poznan Poland: University of Zielona Góra Press.

Nowell, D., Dini, D. and Hills, D. A., 2006, "Recent developments in the understanding of fretting fatigue", Engineering Fracture Mechanics, 73, pp. 207-222.

Talemi, R., H., 2014, "Numerical Modelling Techniques for Fretting Fatigue Crack Initiation and Propagation", Universiteit Gent.

Thomas, A., El-Wahabi, M., Cabrera, J. M., Prado, J. M.. 2006, "High temperature deformation of Inconel 718", Journal of Materials Processing Technology, 177, pp. 469-472.

Vingsbo, O and Söderberg, D., 1988, "On Fretting Maps", Wear, 126, pp. 131–147.

7. RESPONSIBILITY NOTICE

The authors are the only responsible for the printed material included in this paper.